Desease models in vertebrates : from hypoxia to cancer

Santos Marques, I.J. dos

CHAPTER 3

METASTATIC BEHAVIOR OF PRIMARY HUMAN TUMORS IN A ZEBRAFISH XENOTRANSPLANTATION MODEL

Ines J Marques, Frank Ulrich Weiss, Danielle H Vlecken, Claudia Nitsche, Jeroen Bakkers, Anne K Lagendijk, Lars Ivo Partecke, Claus- Dieter Heidecke, Markus M Lerch and Christoph P Bagowski

Article published in ***BMC Cancer*** **2009, 9:128**

All supplemental material can be found online on:

http://www.biomedcentral.com/1471-2407/9/128/additional/

Abstract

Aberrant regulation of cell migration drives progression of many diseases, including cancer cell invasion and metastasis formation. Analysis of tumor invasion and metastasis in living organisms to date is cumbersome and involves difficult and time consuming investigative techniques. For primary human tumors we establish here a simple, fast, sensitive and cost-effective *in vivo* model to analyze tumor invasion and metastatic behavior.

We fluorescently labeled small explants from gastrointestinal human tumors and investigated their metastatic behavior after transplantation into zebrafish embryos and larvae. The transparency of the zebrafish embryos allows to follow invasion, migration and micrometastasis formation in real-time. High resolution imaging was achieved through laser scanning confocal microscopy of live zebrafish.

In the transparent zebrafish embryos invasion, circulation of tumor cells in blood vessels, migration and micrometastasis formation can be followed in real-time. Xenografts of primary human tumors showed invasiveness and micrometastasis formation within 24 hours after transplantation, which was absent when non-tumor tissue was implanted. Furthermore, primary human tumor cells, when organotopically implanted in the zebrafish liver, demonstrated invasiveness and metastatic behavior, whereas primary control cells remained in the liver. Pancreatic tumor cells showed no metastatic behavior when injected into cloche mutant embryos, which lack a functional vasculature.

Our results show that the zebrafish is a useful *in vivo* animal model for rapid analysis of invasion and metastatic behavior of primary human tumor specimen.

Introduction

Approximately 90% of all cancer deaths arise from the metastatic spread of primary tumors (Jemal, et al., 2007). Metastasis formation is a complex, multi-step process in which primary tumor cells invade neighboring tissues, enter the systemic circulation (intravasate), translocate through the vasculature, arrest in distant capillaries, extravasate into the perivascular tissue, and finally proliferate from micrometastasis into macroscopic secondary tumors (Fidler, 2003). Invasiveness and early formation of metastases are the main reasons why for example pancreatic cancer continues to have a dismal prognosis, with a 5 year survival rate of <5% and a mean life expectancy of <6 month (Jemal, et al., 2007).

Zebrafish and their transparent embryos have been employed in several useful models for therapeutic drug research and preclinical studies (Zon, et al., 2005). High throughput screening (HTS) in zebrafish embryos has been established and is nowadays commonly used for different applications (Zon, et al., 2005; Kari, et al., 2007; den Hertog, 2005). A number of unique features make this animal model very attractive: zebrafish are inexpensive to maintain, breed in large numbers, develop rapidly *ex vivo*, and can be maintained in small volumes of water (Parng, et al., 2002). Recently, the zebrafish and its transparent embryos have also come into view as a new model system to investigate tumor development, cancer cell invasion and metastasis formation (Goessling W, 2007; Hendrix, et al., 2007; Grunwald DJ, 2002; Langenau, et al., 2003; Stoletov, et al., 2007). Mary Hendrix and her group have pioneered the field of cancer cell transplantation in zebrafish embryos and could show that transplanted human malignant melanoma cells are not rejected, but survive and even exhibit motility (Lee, et al., 2005; Topczewska, et al., 2006). Haldi *et al.* observed the formation of tumor-like cell masses when xenotransplanting human melanoma cells in

slightly older zebrafish embryos (Haldi, et al., 2006). Several independent studies have now shown that human melanoma cells and other cancer cell lines are able to induce neovascularization when xenografted in the zebrafish (Stoletov, et al., 2007; Haldi, et al., 2006; Nicoli, et al., 2007; Nicoli, et al., 2007).

The role of the small GTPase RhoC in tumor formation, angiogenesis and cell invasion was investigated in real-time in 1-month-old immunosuppressed zebrafish xenografted with the human breast cancer cell line MDA-435 (Stoletov, et al., 2007). This study achieved high-resolution imaging of the dynamic cell-vascular interface in transparent juvenile zebrafish. All these innovative studies established the use of the zebrafish xenotransplantation model for the analysis of cancer cell lines. In this study we now show that zebrafish embryos can even be used to directly transplant human tumor tissue and primary human tumor cells. Zebrafish embryos thus provide a simple, fast and cost-effective method to test the metastatic behavior of primary tumors in an *in vivo* vertebrate animal model that also permits high throughput drug screening.

Methods

Animal care and handling

Zebrafish (*Danio rerio*) (Tuebingen line, *alb* strain (Albinos) and Tg(fli1:eGFP) were handled in compliance with local animal care regulations and standard protocols of the Netherlands and Germany. Fish were kept at 28°C in aquaria with day/night light cycles (10h dark versus 14h light periods). The developing embryos were kept in an incubator at constant temperatures. The cloche (clo) mutant line has been previously described (Herpers, et al., 2008). Heterozygous fish (clo-/+) are kept and bred under normal conditions. 25% of offspring will consist of homozygous clo-/-mutants who lack functional vasculature and

circulation 75% will be siblings with no phenotype. Lack of circulation, an enlarged pericardium and curvature of the tail (at a later time point) are hallmarks of the cloche phenotype.

Cell culture

EpRas cells were cultured at 37°C in DMEM high glucose containing L-glutamine, 4% FCS and 1:100 Pen/Strep (GIBCO, Invitrogen). PaTu8988T and PaTu8898S cells were cultured in DMEM high glucose, with 10% FCS and 1:100 Pen/Strep. The EpRas cells were treated with recombinant human TGF-β1 (RD systems) at a final concentration of 2ng/ml. To induce epithelial to mesenchymal transition (EMT), cells were seeded at 70% confluence in 6-well plates and media containing TGF-β1 (2ng/ml final concentration) was added and replaced every other day for 10 days. After this period, cells were ready for injection.

Cell staining, injections and incubations

Cells were stained with either CM-DiI (red fluorescence) or DiO (green fluorescence) (Vybrant, Invitrogen). Cells were seeded in 6-well plates, grown to confluence trypsinized (without EDTA for EpRas cells or with EDTA for all other cells used). Subsequently, cells were washed with 67% DPBS (GIBCO, Invitrogen), transferred to 1.5ml Eppendorf tubes and centrifuged 5min, at 1500rpm. Cells were re-suspended in DPBS containing either CM- DiI (4ng/µl final concentration) or DiO (200µM final concentration). Cells stained with CM-DiI were incubated 4 min at 37°C and then 15 min at 4°C. Cells stained with DiO were incubated 20min at 37°C. After this period cells were centrifuged 5 min at 1500 rpm, the supernatant discarded and cells re-suspended in 100% FCS, centrifuged again and washed 2 times with 67% DPBS. Cells were suspended in 67% DPBS for

injection into the embryos. 2 dpf zebrafish embryos were dechorionated and anesthetized with tricaine (Sigma). Using a manual injector (Eppendorf; Injectman NI2), the cell suspension was loaded into an injection needle (15µm internal and 18 µm external diameter). Cells were now injected in 2dpf albino or Tg(fli1:eGFP) zebrafish embryos. After injection, embryos were incubated for 1 h at 31°C and checked for cell presence at 2hpt. Fish with fluorescent cells outside the implantation area at 2hpt were excluded from further analysis. All other fish were incubated at 35°C for the following days.

Tissue preparation for transplantation into zebrafish embryos

Human material from surgical resection specimens was obtained at the Universitätsklinikum Greifswald according to local ethical guidelines and after obtaining informed patient consent. Tumor tissue and control tissue were cut into very small pieces using a scalpel blade. A piece of tissue was then transferred to a 2ml Eppendorf tube, washed with 67% DPBS and stained with 1:500 CM-DiI. The tissue was incubated for 6min at 37°C and 20 min at 4°C. Washing procedures were the same as mentioned above for the cells. Before transplantation small pieces of stained tissue were further disaggregated using Dumont forceps (No.5) into a relative size of 1/5 to 1/2 the size of the yolk. Tissue pieces with the correct size were transferred to agarose plates in which the embryos were laying, ready for transplantation. For tumor and control transplantations, a glass transplantation needle was used to transfer the tissue into the yolk. With the glass transplantation needle a piece of tissue was picked up, put on top of the yolk and then pushed inside. The yolk usually sealed itself and in the majority of embryos, the tumor remained in the yolk. After

transplantation, embryos were incubated for 1h at 31°C, and then embryos were checked for presence of tissue and incubated at 35°C for the following days.

Cell dissociation from tissue

Tissue samples were cut in very small pieces using a scalpel blade. Cut tissue pieces were then transferred to 6ml glass containers with 3ml isolation media (180ml DMEM high glucose, 20ml 100 mM HEPES, 46 ml 5% BSA) and Collagenase (Invitrogen) (50µl of a 6mg/ml stock solution for each 12ml of isolation media). Tissue was incubated in a water bath for 15min at 37°C. The supernatant was decanted and tissue pieces were cut further into smaller pieces using a scalpel blade. Tissue pieces were again incubated 15min at 37°C in 3ml isolation media with collagenase. Afterwards tissue pieces were transferred to 15ml falcon tubes and cells were dissolved by pipetting up and down through serial cut blue pipette tips (5 different diameters). The cell suspension was now filtered through 2 sheets of gaze, into 2ml Eppendorf tubes and centrifuged 5min at 1500rpm. The supernatant was discarded and cells re-suspended in isolation media. The described procedure was then repeated once. For injections, cells were stained with either CM-DiI or DiO and injected into 2dpf zebrafish embryos, as described above.

Western-Blotting

Pancreatic cancer cell lines PaTu-S and PaTu-T were lysed in iced Triton-X-100 lyses buffer (0.1%) containing protease inhibitors (1ml/mg tissue, 10µg/ml aprotinin, 10µg/ml leupeptin, 0,01M sodiumpyrophosphate, 0,1M sodiumfluoride,

1mM dihydrogenperoxide, 1mM L-phenylmethylsulfonylfluoride [PMSF] and 0,02% soybean-trypsin inhibitor). Protein concentration was determined by a modified Bradford-assay (Bio Rad Laboratories, München, Germany) and equal amounts of protein were used in subsequent experiments. Cell lysates were separated by SDS-PAGE on a 7.5% polyacrylamide gel in a discontinuous buffer system and gels were blotted on nitrocellulose membranes (Hybond C, GE Healthcare Europe GmbH). After overnight blocking in NET-gelatin (10mM Tris/HCl pH 8.0, 0.15mM NaCl, 0.05% Tween 20, 0.2% gelatin) immunoblot analysis was performed followed by enhanced chemoluminescence detection (GE Healthcare Europe GmbH) using horseradish peroxidase coupled sheep anti-mouse IgG or goat anti-rabbit IgG GE Healthcare Europe GmbH). Monoclonal E-cadherin antibody (Clone 36), directed against the carboxy-terminus, was purchased from Transduction Laboratories (San Diego, CA, USA) as well as antibodies against α-, β-, and γ-Catenin. A polyclonal G3PDH antibody was purchased from Biozol (Eching, Germany).

Immunofluorescence microscopy

PaTu-S and PaTu-T cells grown on glass coverslips for 24–48 h were washed 3 times with PBS, fixed for 15 min in 4% paraformaldehyde and permeabilised in 0.1% Triton-X-100 for 5 min. Blocking of unspecific binding was achieved by a 1 h incubation in 10% Aurion BSA-c (Aurion, Waageningen, The Netherlands). Following a primary antibody incubation overnight (dilutions 1:100) and subsequent PBS washing steps detection was per-formed using dichlortriacinyl aminofluoresceine (DTAF) or Cy3-coupled sheep IgG (dilutions 1:200). Nuclei were stained by 30 sec. incubation with DAPI (1:10000 in PBS). After a final washing step in PBS cell were mounted in Vectashield (Vector Labs, Burlingame,

CA, USA). Microscopic Images were taken using an AxioCam digital microscope camera on a Zeiss Axiophot microscope.

In vitro migration assay ("scra*tch"-assay*)

The scratch-assay was performed as previously described by Liang *et al.* (2007). Cells were grown to confluence in 6-well dishes and mitomycin C was added at 10 µM for 2 h. Then the cell monolayer was scraped in a straight line with a 200 µl pipette tip. Pictures of the scratch were taken under an invert Olympus microscope at 0h, 12h and 24h.

Histology of zebrafish embryos

Transvers sections at 4 µM thickness were prepared as described before (te Velthuis, et al., 2007). Sections were directly imaged with fluorescence microscopy or differential interference (DIC) microscopy. After fluorescent pictures were taken, Haematoxylin/Eosin (HE) staining was performed as described earlier (Marques, et al., 2008).

Whole mount immunofluorescence of zebrafish embryos

Zebrafish embryos at 2 dpt were fixed overnight in 4%PFA in PBS at 4°C. After fixing, embryos were washed with BSAc 0.1%-TritonX100 1% in PBS (blocking buffer; 3x10 minutes). Subsequently, the embryos were incubated for 2h in blocking buffer at RT. Incubation with the primary antibody (Mouse anti-Proliferating Cell Nuclear Antigen, PCNA, from Zymed Laboratories, 1:100) was done overnight at 4°C. After washing (3 × 10 minutes) with blocking buffer, embryos were incubated with the secondary antibody (Fluorescein (DTAF)-conjugated AffiniPure Goat anti-Mouse IgG, Jackson Immuno Research

Laboratories, Inc., 1:100) for 1h and washed afterwards with blocking buffer (3×10 minutes). Embryos were mounted in 3% methylcellulose to orient them properly for imaging. Imaging was done with confocal scanning laser microscopy (Biorad 1024ES; Software: Biorad Laser sharp 2000).

Imaging, selection and positioning of transplanted zebrafish embryos

Confocal pictures were taken either with the Biorad Confocal microscope 1024ES (Zeiss microscope) combined with Krypton/Argon laser, or the dual laser scanning confocal microscope Leica DM IRBE (Leica) or with the Nikon TE300 confocal microscope and a coherent Innova 70C laser (Chromaphor, Duisburg, Germany). Pictures were further taken by DIC microscopy using the Axioplan 2 microscope with an AxioCam MR5 camera (Carl Zeiss). Further, fluorescent stereomicroscope pictures were taken with the Leica DFC 420C camera attached to a Leica MZ16FA microscope. Two hours post implantation the embryos were anesthetized with tricaine and positioned laterally, with the site of the implantation to the top, on 3% methylcelulose, on a slide with depression. Each time two rows of twenty embryos were screened. Two hours post implantation every embryo that showed cells outside the area of implantation were discarded and not considered for the experiment.

Results

Tumor cell xenografts in zebrafish embryos

Mouse mammary epithelial cells (EpH4), transformed with oncogenic Ras (EpRas), have been used to establish a mouse tumorigenesis model over a decade ago (Oft, et al., 1996). In these EpRas cells, TGF-β signaling causes epithelial to mesenchymal transition (EMT) which transforms cells to a highly invasive phenotype and enables distant metastasis formation when transplanted

into nude mice (Oft, et al., 1998). Initially, we evaluated metastasis formation using this well characterized system in the zebrafish cell xenograft model. We transplanted fluorescently labeled EpRas cells into the yolk sac of 2 day old zebrafish embryos to study metastatic behavior *in vivo*. EpRas cells that had been stimulated with TGF-β for 10 days prior to injection, showed metastatic behavior in the zebrafish, comparable to results previously reported in mice (Oft, et al., 1998; Oft, et al., 1996; Waerner, et al., 2006). Following EMT the cells invaded embryonic tissue, entered the circulation and homed in at distant tissues and organs. EpRas TGFβ treated cells were found in blood islands, brain, caudal fin, caudal vein, gill arches, heart, intestine, liver, mandible, optic cup (eye), otic cup, pericardium, somites, swim bladder. However, they had a tendency to invade and home in to muscle tissue, head structures, caudal fin and blood islands (Figure. 1 and Additional File 1). To a lesser extent, we observed invasion of these cells into the liver or other organs of the gastrointestinal tract. In contrast, non-stimulated EpRas control cells remained at the place of injection in the yolk and neither did not invade the developing zebrafish nor did they enter blood circulation (Figure. 1 and Additional file 2). In three independent experiments the average percentage of migrating cells observed for the EpRas TGF-β-stimulated cells was 46.6% (SD±2.0; p-value < 0.001) compared to 0.5% (SD± 0.7; p-value<0.001) for the parental EpRas cells (see Additional file 1). Furthermore, the TGF-β stimulated EpRas cells formed tumor cell masses in the developing zebrafish (Figure. 1), which resemble the formation of metastases in nude mice (Waerner, et al., 2006). In the zebrafish, cells begin to invade the embryo already several hours after injection (on average 4 hours post injection) (see Additional File 3) and tumor cell masses are visible as early as 3 days post implantation (dpi).For optimal visualization, we used the transgenic zebrafish line,

Tg(fli1:eGFP) (Stoletov, et al., 2007; Waerner, et al., 2006), which expresses GFP under the *fli1* promoter (an early endothelial marker) and therefore exhibits a green fluorescent vasculature (Stoletov, et al., 2007; Lawson, et al., 2002). In a time lapse movie (see Additional file 4; rate: 1 frame/ minute) we show an example of fluorescently labeled EpRas TGF-β cells (3 dpi) which have invaded the zebrafish body, have translocated into the vasculature and have colonized at distant sites in the zebrafish larvae (5 dpf). Some cells are visible in the blood stream whereas others have extravasated from the vasculature. Evaluation of metastasis formation in the zebrafish model is therefore significantly faster than in currently used mouse models, where it may take several weeks until metastases become detectable (Waerner, et al., 2006). The sensitivity of the zebrafish tumor xenograft model further allows observation of individual cells and their daughter cells *in vivo*.

We also compared the two established human pancreatic tumor cell lines, PaTu8988-S and PaTu8988-T (Elsässer HP, 1992) (referred to herein as PaTu-S and PaTu-T) in their invasive and metastatic potential in a single zebrafish. Both sister cell lines originate from liver metastases of the same human pancreatic adenocarcinoma (Elsässer HP, 1992). E-Cadherin expression in PaTu-S cells (Figure 2A and 2B (a)) correlates with the maintenance of functional cell-cell contacts (Figure 2B) and a reduced tendency of cells to migrate (Figure2C) (Menke, et al., 2001; Mayerle, et al., 2005). Whereas PaTu-S cells show localization of E-cadherin/β-catenin complexes at the plasma membrane (Figure 2B (e)), PaTu-T cells lack E-Cadherin expression (Figure 2A and 2B (b)) and β-catenin is mainly localized in the cytoplasm (Figure 2B (d). This observation is paralleled by enhanced migratory capabilities of PaTu-T cells compared to PaTu-S

cells, which we confirmed in an *in vitro* migration assay ('scratch assay' (Cha, et al., 1996) (Figure 2C and Additional file5).

We then labeled PaTu-S cells with green fluorescence and PaTu-T cells with red fluorescence. When implanted successively in the yolk sac of the same zebrafish embryo, green PaTu-S cells remained in the yolk, whereas red PaTu-T cells displayed invasion and metastatic behavior (Figure 2D and Additional file 1). Similar results were observed when cells were mixed prior to injections (data not shown).

PaTuT cells were found in the brain, caudal vein, gill arches, gut, heart, intestine, liver, operculum, pericardium, somites, and swim bladder. They showed a tendency to invade and home in to organs of the gastrointestinal tract. Micrometastasis was often observed in organs such as the liver, the gut and the intestine. Invasion and homing of these cells into muscle tissue was observed to a lesser extent. This behavior was qualitative different from what we observed for TGF-β treated EpRas cells. We further tested the metastatic behavior of PaTu-T cells in homozygous *cloche* mutants (cloche$^{-/-}$), which lack a functional vasculature and circulation (Herpers, et al., 2008) Additional File 6). In contrast to control zebrafish, no metastatic behavior was observed in the cloche$^{-/-}$-fish, indicating that the observed invasion/migration of PaTu-T cells indeed involves metastasis formation through the vascular sys- tem. Zebrafish were followed until three days post injections (Figure 2E; see Additional files 1 and 7).

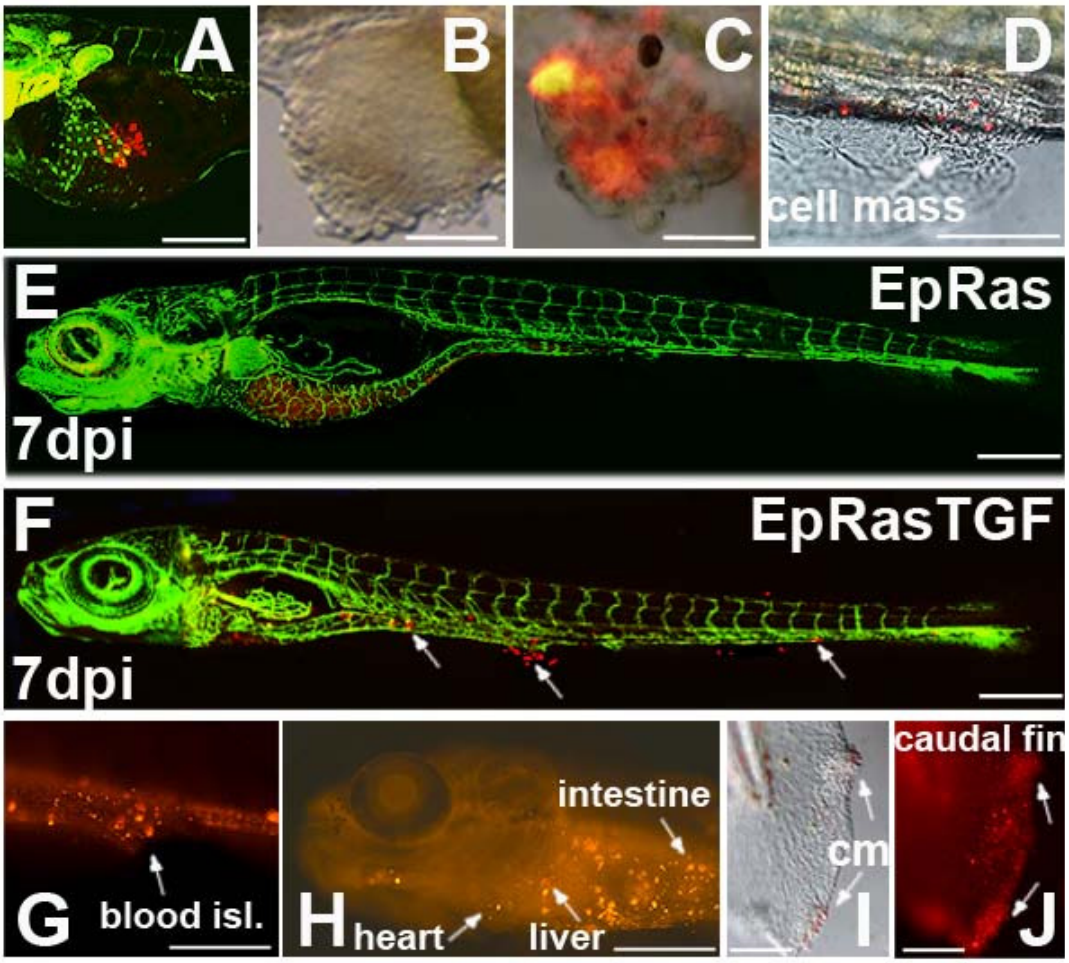

Figure 1 Migration and cell mass formation of Ha-Ras transformed mouse mammary epithelial cells injected into the yolk sac of zebrafish embryos. EpRas (parental) and EpRas cells stimulated with TGF-β (EpRasTGF) were labeled and ectopically injected into the yolk sac of 2 dpf zebrafish embryos. In A, E and F transgenic zebrafish embryos expressing GFP under an endothelial promoter (Tg(fli1:eGFP) were used. An example of newly injected EpRas cells at 1 hour post injection is given in (A). In (B) an ectopic tumor cell mass formed in the yolk sac by EpRasTGF cells is shown. Examples of cell masses formed by EpRasTGF cells at distance from the place of injection are shown for the tail region (C) and blood islands with surrounding ventral fin (D). Pictures in B-D were taken at 3 dpi. While EpRas cells

remained in the yolk and never invaded the embryo (E), EpRasTGF cells invaded, migrated and formed distant micrometastasis, which are indicated with arrows (F). Red fluorescence of cells is still visible after 7 dpi (E, F).Images G to J show tumor cell masses (cm) and migrated cells in blood islands (blood isl.), the liver, heart, intestine and the caudal fin of 6 dpi larvae. Scales shown are for A: 200 µm; D-H: 600 µm, for B, C, I and J: 100 µm. 3D reconstructions of EpRAS and EpRasTGF cells in zebrafish larvae are shown in two supplemental movies (see Additional files 2 and 3).

Human tumors transplanted into zebrafish display metastatic behavior

We then pursued our primary goal to employ the zebrafish also as a simple, fast and effective test system for metastasis formation of primary human tumors. After informed patient consent small fragments of tumor explants from pancreas, colon and stomach carcinoma, as well as tumor free areas from the same resection specimen were fluorescently labeled with CM-DIL and directly xenotransplanted into the yolk sac of zebrafish embryos. Tumor and non-tumor control cells were followed live by laser scanning confocal microscopy.

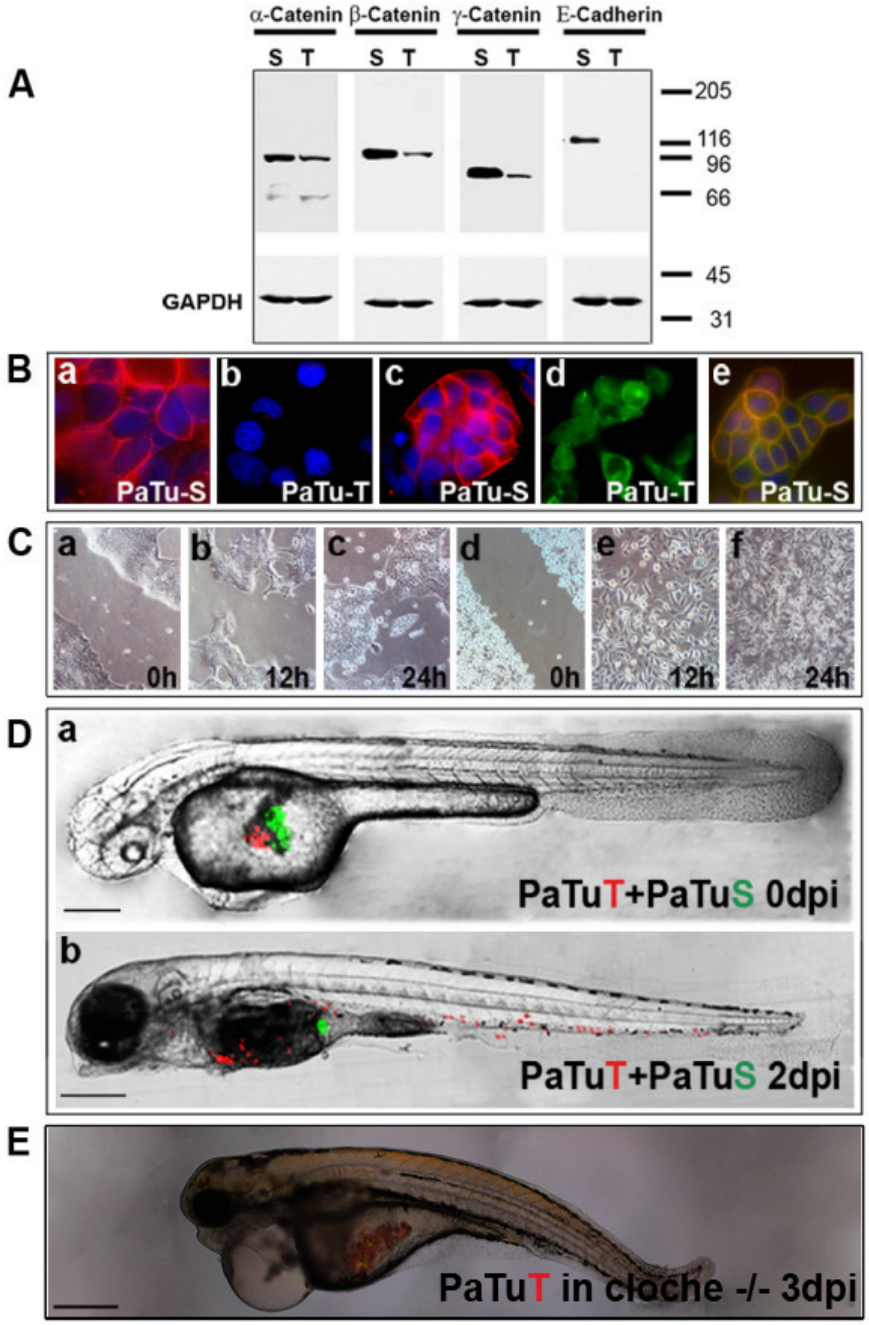
A
α-Catenin
β-Catenin
γ-Catenin
E-Cadherin
S T S T S T S T
205
116
96
66
45
31
GAPDH
B
a
PaTu-S
b
PaTu-T
c
PaTu-S
d
PaTu-T
e
PaTu-S
C
a
0h
b
12h
c
24h
d
0h
e
12h
f
24h
D
a
PaTuT+PaTuS 0dpi
b
PaTuT+PaTuS 2dpi
E
PaTuT in cloche -/- 3dpi

Figure 2 Implantation of two pancreatic cancer cell lines into the same zebrafish embryo. **(A**) Western blot analysis shows that PaTu-S but not PaTu-T cells express E-cadherin and both express α-, β- and γ-catenin. GAPDH expression is shown as a control. (**B**) Cellular localization of E-cadherin and β-catenin was analyzed by immunofluorescence. E-cadherin expression is shown for PaTu-S cells (a) and absence of E-cadherin expression for PaTu-T cells (b). Dapi staining was used to visualize cell nuclei in blue. β-catenin localization is shown for PaTu-S (c) and for PaTu-T (d). Co-localization of E-cadherin (green) and β-catenin (red) in PaTu-S cells is indicated by yellow staining of the plasma membrane (e). (**C**) An in vitro migration assay ('scratch assay') shows differences in migration of the two cell lines (PaTu-S: a-c and PaTu-T: d-f). Similar results were obtained in four independent experiments. Gap closure (gap width) over time is shown in Additional file 5. (**D**) Non-invasive PaTu-S cells (green) and invasive PaTu-T cells (red) were implanted consecutively in the same embryo (a and b) (Scales: 250 µm (a) and 300µm (b)). (**E**) Homozygous cloche mutants [17] were injected with PaTu-T cells and followed over time. Shown is an example of a cloche$^{-/-}$ zebrafish at 3 dpi (scale bar: 300 µm). In contrast to control zebrafish none of the tested cloche$^{-/-}$mutants showed any sign of metastatic behavior (see Additional file 1 and Additional file 7). The cloche phenotype and its lack of a functional vasculature and circulation is observable by DIC microscopy (see Additional file 6).

Tumor cells started to invade the embryo on average 12 hours post injection and micrometastasis formation was visible as early as 24 h post injection. In parallel, we also investigated and compared the invasive and metastatic behavior of tumor cells that had been dissociated from primary human tumors by collagenase digestion prior to transplantation.

In total, pancreatic tumors of four different patients were analyzed. Three had carcinomas of the pancreas head and one had an adenocarcinoma of the ampulla vateri with infiltration of the pancreas (cancer grades and pTMN stages

for all tumors are shown in table 1). On average 59.8% (SD±5.2) of transplanted pancreatic tumor fragments showed invasion and migration in the developing zebrafish (table 1 and Figure 3).

Evaluation criteria for invasion and migration were that at least 5 cells had to be identified outside of the yolk and detectable within the developing zebrafish (table 1). Development of micrometastasis was assessed by the presence of daughter cells at 3dpt. The results are listed in table 1 and in Figure 4 examples of micrometastasis in different tissues detected in sections of 5dpf zebrafish are shown at high resolution (Figure 4B, C, D, G, H, K and 4L). An example showing proliferating pancreatic tumor cells and the initial formation of a micrometastasis is given in Figure 5(E). Cell division is further indicated by PCNA immunostaining of invasive tumor cells in the zebrafish embryo (see Additional file 8). After 5dpf embryos fall under strict local animal experiment regulations, therefore most embryos were not followed for longer periods. It is likely that the number of micrometastasis would still increase over time.

Invasive cells were found for pancreatic tumors in blood islands, caudal fin, caudal vein, gut, heart, hindbrain, intestine, liver, mesonephric duct, mesonephric tubule, mandible, operculum, pericardium, somites, swim bladder, for the colon tumor in caudal vein, gut, heart, intestine, liver, pericardium; and for the stomach tumors in the caudal vein, gill arches, heart, intestine, liver, *mandible, otic cup, pericardium.*

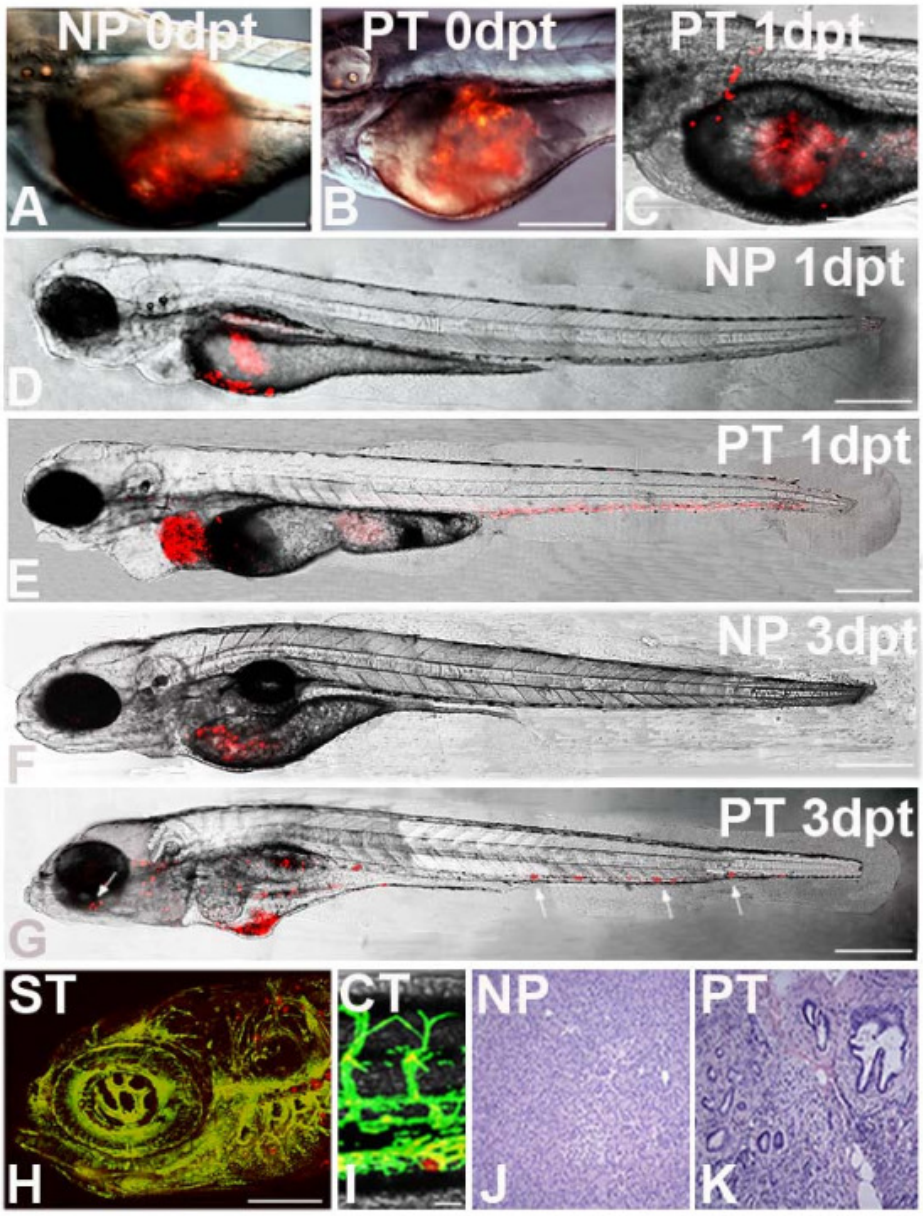

Figure 3 Tumor transplantation in zebrafish. Primary human tumours of the pancreas,

the stomach and the colon were transplanted into 2 dpf embryos. Non-tumour tissue was used as control. At the respective time points indicated laser confocal microscopy images were taken. Images A and B show newly transplanted embryos with normal pancreas (NP) and pancreatic tumour (PT) respectively. Image C shows an example of an embryo transplanted with an adeno-carcinoma of the pancreas at 1 day post transplantation (dpt) in which tumour cells have already invaded the embryo. Images D to G are confocal microscopy images of transplanted embryos at 1 dpt and 3 dpt. Normal, non-transformed pancreas transplants remain in the yolk and cells never migrate or spread in the embryo (D and F). In contrast, tumour transplants show metastatic behaviour (E and G). Some of the cell masses are marked with arrows, including one formed near the retina of the eye (G). On the bottom an example is shown for brain metastases of a transplanted gastric cancer (stomach tumour) in a Tg(fli1:eGFP) zebrafish 3 days after implantation(H). Cell masses are visible in the rhombencephalon (hindbrain) surrounding the otic capsule and near the gill arches (H). A colon tumour transplant shows a migrated tumour cell in the caudal vein region at 3 dpt (I). Both pictures (H and I) were taken by confocal microscopy. HE staining of representative histological sections of normal human pancreas tissue (J) and pancreatic cancer (K) are shown. Scales shown are in A-E: 300 μm; F, G: 400 μm; in H: 100 μm and in I: 20 μm.

Similar to preferences observed for PaTu-T cells, tumor cells of implanted gastrointestinal tumor tissue fragments had a tendency to invade and home in to organs of the gastrointestinal tract. Micrometastasis was often observed in the liver, the gut and the intestine. Homing of these cells in muscle tissue and the formation of micrometastasis was rarely observed. Although we observed qualitative differences for the preferential homing of the two cell lines tested (PaTu-T and TGF-β treated EpRAS cells), a future study, with a larger cohort of

tumor specimen and tumor types is necessary to determine tumor specific preferences.

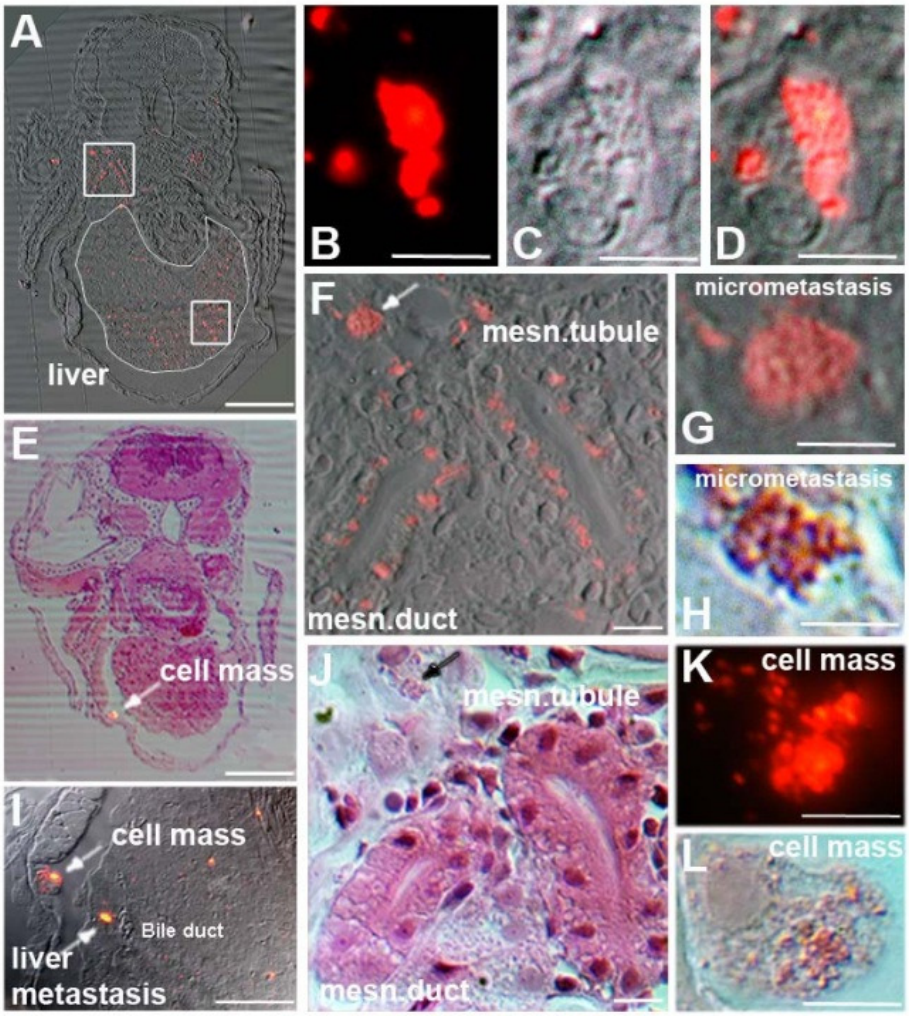

Figure 4 Histology of zebrafish embryos transplanted with a human pancreatic tumor. Transversal sections of zebrafish embryos trans-planted with a primary human pancreatic

tumor show the presence of micro-metastases in different tissues at 3 dpt in 5 day old zebrafish. (A) The transversal section is approximately 40 µm caudal to the anterior end of the liver. The liver is circled with a thin white line and contains many tumor cells and some micrometastases. The square in the liver contains several micrometastases, of which one is depicted in higher magnification in B (fluorescence), C (DIC) and D (overlay). The upper square shows tumor cells and micrometastases around the mesonephric tubule (msn. tubule) and the mesonephric duct (msn. duct). The enlargement of the square is shown in F and J (HE staining). In both, F (white arrow) and J (black arrow) micrometastasis is indicated (high magnifications in G and H). In (E) HE staining of a transversal section approximately 24 µm rostral to the anterior start of the liver is shown and overlaid with the fluorescent image. A larger cell mass is indicated by an arrow. The same cell mass is indicated in I in which also a liver metastasis is seen. The cell mass is shown in high magnification in K (fluorescent picture) and in L (HE staining). Scales shown are A and E 1 mm, B-D, F-H and J-L 10 µm and in I: 500 µm.

Figure 3 shows examples of fish embryos directly after transplantation (A, B) and at 1 and 3dpt (C-G). Cell invasion and micrometastasis formation of pancreatic tumor cells is clearly detectable 24 h after transplantation (E). Similar results were also obtained for transplanted tissue fragments of a colon adenocarcinoma (43.9% invasion and migration) and two moderately differentiated adenocarcinomas of the stomach (average 53.5%, SD±1.2) (p-values in all tumor experiments were <0.001). As a control for the tumors we used colon and gastric mucosal fragments or peritumoral, non-transformed tissue of the respective tissue explants from the same patients. In the pancreas the non-transformed tissue controls mostly showed histological manifestations of chronic pancreatitis and only one was considered as having a normal pancreatic histology.

Histological sections of control pancreas and of pancreatic cancer tissue of human patients are shown in Figure 3(J, K). In all control transplantations of chronic pancreatitis specimen and of fragments of normal pancreas, colon and stomach tissue cellular invasion and migration was never observed (see Additional file 1 and Figure 3D, F). In addition, we also tested the metastatic behavior of a benign tumor. Tissue fragments of adenomateous colonic polyps (0,4cm and 1cm) were investigated, which had not yet invaded through the lamina muscularis mucosae. No metastasis was observed for either of them in the zebrafish embryo (Additional file 1). Comparable results were seen when cells were dissociated from tumor or control tissue samples prior to their injection into the zebrafish. All four primary pancreatic tumor cells showed cellular invasion and migration with an average of 48.8% (SD±9.0) (see Additional file 1). In the case of dissociated primary colon and stomach tumor cells 44.4% and 35.3% of cell injections, respectively, resulted in cellular invasion and migration (see Additional file 1).

Xenotransplantation experiments of tumor fragments as well as the injection of isolated primary tumor cells allowed discriminating between non-invasive chronic pancreatitis and infiltrating pancreatic adenocarcinoma. In real-time, we show an example of pancreatic tumor cells in the zebrafish 1 day after a pancreatic cancer fragment was transplanted (see Additional file 9). This movie shows circulating tumor cells and tumor cells which have extravasated into the perivascular tissue of a 3 day old zebrafish. A moving primary human tumor cell passing through the caudal vein and into an intersegmental vessel is also visible. In a supplemental movie we show how a pancreatic tumor cell is slowly traversing through the caudal vein of a 3 dpt Tg(fli1:eGFP) zebrafish (see Additional file 10). In Figure 4 histological sections of zebrafish embryos

transplanted with a pancreatic human tumor are shown at 3 dpt. Examples of micrometastasis in the liver (B, C and D) and near the mesonephric duct (G and H) are shown at higher magnifications. A cell mass is further shown in K and L.

Organotopic transplantation of primary human tumor cells in the fish liver and the effects of protease inhibitors on the invasiveness of implanted tumor cells and tumor fragments

Some xenograft models that have been established in the mouse involve the orthotopic transplantation of specific human tumors and tumor cells (Sharpless, et al., 2006; Frese, et al., 2007). Surgical orthotopic implantations (SOI) of tumor cells or of resected primary tumor fragments into immune deficient mice have proven useful for studying their growth and metastatic potential (Hoffman, 2005).

Here we transplanted freshly dissociated primary pancreatic tumor cells and normal pancreatic control cells into the liver of zebrafish larvae. For these experiments, we used the Tg(fli1:eGFP) transgenic zebrafish line (with the advantage of a fluorescent vasculature), which allows an exact localization and injection into the highly vascularized liver. Primary cells of control pancreatic tissue, when transplanted into the liver, remained at the site of the injection and did not invade the developing zebrafish nor did they enter the blood circulation (Figure. 5). In contrast, primary tumor cells invaded the neighboring tissue, entered the circulation and migrated and homed in on distant tissues and organs (Figure. 5).

Furthermore we investigated in our zebrafish xenotransplantation model the effects of protease inhibitors on the invasiveness of implanted tumor cells and tumor fragments. Two different protease inhibitors were able to inhibit the

invasiveness of tumor cells and of a primary pancreatic tumor (see Additional file 1).

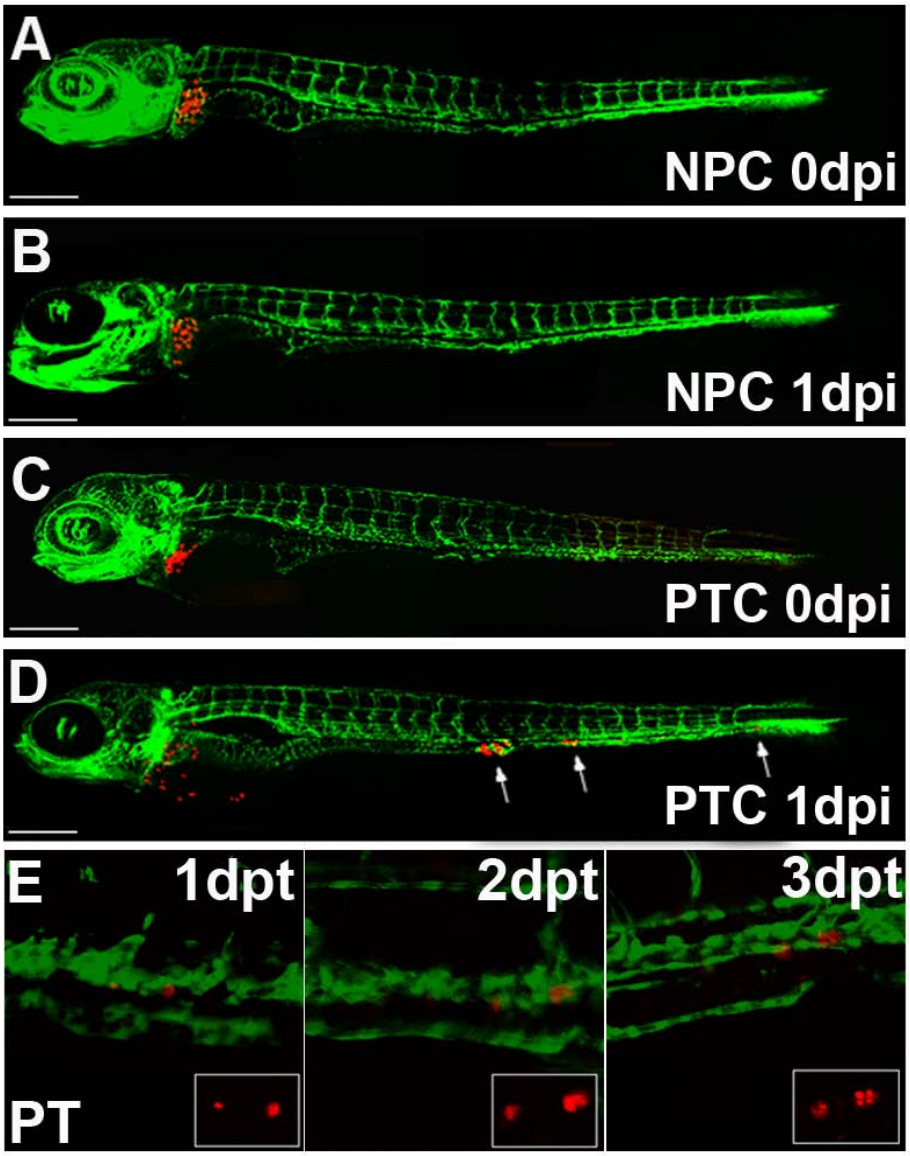

Figure 5 Implantation of primary human tumor cells into the zebrafish liver. (A-D) Organotopic implantation of primary tumor cells into the liver of larvae of Fli-1 zebrafish. Representative examples of zebrafish at 5 days of development injected

with primary normal pancreatic cells (NPC) and with primary dissociated pancreatic tumor cells (A and C, respectively) are shown. The same fish are depicted at 1 day post injection (1 dpi). While normal pancreatic cells remained at the site of implantation in the liver (B), pancreatic tumor cells invaded the embryo and formed distant metastases, indicated with arrows (D). Scales indicated are: A-D 300 □m. Individuals were followed for up to 7 dpi and untransformed control cells never invaded the host embryos and remained in the liver for the entire observation period (data not shown). Image E shows an example of proliferating tumor cells of a transplanted pancreatic tumor fragment on consecutive days. The single cell on the right seen at 1 day post transplantation is divided into two daughter cells on 2 dpt and four cells are visible at 3 dpt. Dual color laser scanning confocal images of the Fli-1 zebrafish are shown and in the smaller insert the red fluorescence of the CM-DiI labeled tumor cells can be seen.

Discussion

Analysis of tumor metastasis in an in vivo model depends on intrinsic tumor cell properties, host factors and the experimental techniques used. The engraftment of human neoplasms in the mouse normally requires the use of nude (athymic) or severe combined immune deficient (SCID) mice that are T-and B-cell deficient. In these animal models further attention has to be paid to the site of implantation, as host factors may differ between tissues and organs. Nude mice also have an upregulated innate immunity and elevated numbers of natural killer cells and tumoricidal macrophages, which may limit tumor growth or even prevent metastasis. Efficacy of pharmacological and toxicological studies in murine xenograft models normally use tumor growth, body weight loss and mortality as parameters of toxicity. These studies are cumbersome, time consuming and drug activity against xenografts does not always correlate with its clinical activity (Johnson, et al., 2001).

In our study we established the zebrafish as a robust *in vivo* model for investigating invasiveness and metastatic behavior of human primary tumors. It is known that early zebrafish embryos do not reject xenotransplanted human cells (Topczewska, et al., 2006; Haldi, et al., 2006; Nicoli, et al., 2007), whereas 1 month old zebrafish already need to be immune suppressed (Stoletov, et al., 2007).

The early embryos and larvae used here did not reject the primary tumor xenografts, most likely due to the fact that their immune system is not fully developed. It has been observed that while lymphopoiesis and lymphoid organogenesis are initiated at the middle to late embryo period, they remained in their rudimentary and immature form throughout the early larval stages. The major maturation events leading to immune competence occur between 2 and 4 weeks post fertilization (wpf), coinciding with the larval to juvenile transitory phase (Lam, et al., 2004).

The observed metastasis in an animal model primarily should reflect the intrinsic metastatic ability of the tumor cells, but may depend to some extent also on the experimental system. Other experimental animal systems have demonstrated that only a small subset of metastatic cells (approximately 2%) survive and grow at secondary sites (Weiss, 1990). The significantly higher percentage of micrometastases observed using fish embryos may in part reflect the absence of the humeral immune response and/or other selective pressures on tumors cells which would lead to tumor cell death following extravasation into secondary organs.

The transparency of the fish embryo enables an investigation of fluorescently labeled tumor cells in real time and at high resolution. The unique availability of transgenic zebrafish without a functional vasculature (Herpers, et al., 2008)

further allowed us to show that the metastatic spread of tumor cells in zebrafish embryos involves the vascular system. Even the very early steps of invasion, circulation of tumor cells in blood vessels, colonization at secondary organ sites and metastasis formation can be observed this way-something which to date cannot be investigated in established mouse tumor models. Advantages of the model system such as good accessibility, easy handling, low costs and short incubation times make it a promising system for future functional studies in primary tumors.

The experiments described here provide the basis for the future development of a screening methodology of drugs, which inhibit invasion and metastasis of human tumors. Recently, adult zebrafish with an almost entirely transparent body have been described, as a novel tool for *in vivo* transplantation analysis (White, et al., 2008). These will be of interest for additional comparative analysis of metastasis formation of primary tumors in the immune competent animal.

Conclusion

We demonstrate here the applicability of the zebrafish embryo as an *in vivo* model for the analysis of metastatic behavior of human tumor cells, including resection specimen from human tissue. High resolution imaging of live zebrafish has and will further assist in better understanding the underlying mechanisms of cancer cell invasion and metastasis formation. Advantages of the model system such as good accessibility, easy handling, low costs and rapidness are unparalleled by other vertebrate organisms and make it a promising system for future functional studies in primary tumors. The advantages of the "short term"

zebrafish embryo model could nicely complement established "longer term" tumor models, e.g. mouse models, and may be a valuable and efficient tool to evaluate novel therapeutic strategies for cancer.

Acknowledgements

We would like to thank G. Posern for supplying the mouse cells, Davy de Witt for his part of animal welfare and Joost Woltering and Jaya Besser for critical remarks on the manuscript. We would further like to acknowledge and thank the Tübingen 2000 Screen Consortium and Exelixis, as the original source of the cloche mutant embryos. This work was supported by grants from the Portuguese foundation for Science and Technology (SFRH/ BD/27262/2006), the Deutsche Krebshilfe (10-2031-Le) and the Alfried-Krupp-Foundation.

References

Jemal A, Siegel R, Ward E, Murray T, Xu J, Thun MJ (2007) *Cancer Statistics, 2007. CA*: A Cancer Journal for Clinician, 57(1):43-66.

Fidler IJ (2003) *The pathogenesis of cancer metastasis: the 'seed and soil' hypothesis revisited.* Nature Reviews: Cancer, 3(6):453-458.

Zon LI, Peterson RT (2005) *In vivo drug discovery in the zebrafish.* Nature Reviews: Drug Discovery. 4(1):35-44.

Kari G, Rodeck U, Dicker AP (2007) *Zebrafish: An Emerging Model System for Human Disease and Drug Discovery.* Clinical Pharmacology Therapy, 82(1):70-80.

den Hertog J (2005) *Chemical Genetics: Drug Screens in Zebrafish.* Bioscience Report, 25(5):289-297.

Parng C, Seng WL, Semino C, McGrath P (2002) *Zebrafish: A Preclinical Model for Drug Screening.* ASSAY and Drug Development Technologies, 1(1):41-48.

Goessling W, North TE, Zon LI: *New Waves of Discovery: Modeling Cancer in Zebrafish.* Journal of Clinical Oncology, 25(17):2473-2479.

Hendrix MJC, Seftor EA, Seftor REB, Kasemeier-Kulesa J, Kulesa PM, Postovit L-M: (2007) *Reprogramming metastatic tumor cells with embryonic microenvironments.* Nature Reviews Cancer, 7(4):246-255.

Grunwald DJ, Eisen JS (2002) *Headwaters of the zebrafish [mdash] emergence of a new model vertebrate.* Nature Reviews: Genetics, 3(9):717-724.

Langenau DM, Traver D, Ferrando AA, Kutok JL, Aster JC, Kanki JP, Lin S, Prochownik E, Trede NS, Zon LI, Look AT (2003) *Myc-Induced T Cell Leukemia in Transgenic Zebrafish.* Science, 299(5608):887-890.

Stoletov K, Montel V, Lester RD, Gonias SL, Klemke R (2007) *High-resolution imaging of the dynamic tumor cell vascular interface in transparent zebrafish.* Proceedings of the Natural Academy of Sciences, 104(44):17406-17411.

Lee Lisa MJ, Seftor EA, Bonde G, Cornell RA, Hendrix MJC (2005) *The fate of human malignant melanoma cells transplanted into zebrafish embryos: Assessment of migration and cell division in the absence of tumor formation.* Developmental Dynamics, 233(4):1560-1570.

Topczewska JM, Postovit L-M, Margaryan NV, Sam A, Hess AR, Wheaton WW, Nickoloff BJ, Topczewski J, Hendrix MJC (2006) *Embryonic and tumorigenic pathways converge via Nodal signaling: role in melanoma aggressiveness.* Nature Medicine, 12(8):925-932.

Haldi M, Ton C, Seng W, McGrath P: Human melanoma cells transplanted into zebrafish proliferate, migrate, produce melanin, form masses and stimulate angiogenesis in zebrafish. Angiogenesis 2006, 9(3):139-151.

Nicoli S, Ribatti D, Cotelli F, Presta M (2007) *Mammalian Tumor Xenograft Induce Neovascularization in Zebrafish Embryos.* Cancer Research, 67(7):2927-2931.

Nicoli S, Presta M (2007) *The zebrafish/tumor xenograft angiogenesis assay.* Nature Protocols, 2(11):2918-2923.

Herpers R, Kamp E van de, Duckers HJ, Schulte-Merker S (2008) *Redundant Roles for Sox7 and Sox18 in Arteriovenous Specification in Zebrafish.* Circulation Research, 102(1):12-15.

Liang C-C, Park AY, Guan J-L (2007) *In vitro scratch assay: a convenient and inexpensive method for analysis of cell migration in vitro.* Nature Protocols, 2(2):329-333.

te Velthuis AJW, Ott EB, Marques IJ, Bagowski CP (2007) *Gene expression patterns of the ALP family during zebrafish development.* Gene Expression Patterns, 7(3):297-305.

Marques I, Leito J, Spaink H, Testerink J, Jaspers R, Witte F, Berg S van den, Bagowski C (2008) *Transcriptome analysis of the response to chronic constant hypoxia in zebrafish hearts.* Journal of Comparative Physiology B: Biochemical, Systemic, and Environmental Physiology, 178(1):77-92.

Oft M, Peli J, Rudaz C, Schwarz H, Beug H, Reichmann E (1996) *TGF-beta1 and Ha-Ras collaborate in modulating the phenotypic plasticity and invasiveness of epithelial tumor cells.* Genes & Development, 10(19):2462-2477.

Oft M, Heider K-H, Beug H (1998) *TGF[beta] signaling is necessary for carcinoma cell invasiveness and metastasis.* Current Biology, 8(23):1243-1252.

Waerner T, Alacakaptan M, Tamir I, Oberauer R, Gal A, Brabletz T, Schreiber M, Jechlinger M, Beug H (2006) *ILEI: A cytokine essential for EMT, tumor*

formation, and late events in metastasis in epithelial cells. Cancer Cell, 10(3):227-239.

Lawson ND, Weinstein BM (2002) *In Vivo Imaging of Embryonic Vascular Development Using Transgenic Zebrafish.* Developmental Biology, 248(2):307-318.

Elsässer H, PL U, Agricola B, Kern HF (1992) *Establishment and characterization of two cell lines with different grade of differentiation derived from one primary human pancreatic adenocarcinoma.* Virchows Archive B: Cell Pathology Including Molecular Pathology, 61(5):295-306.

Menke A, Philippi C, Vogelmann R, Seidel B, Lutz MP, Adler G, Wedlich D (2001) *Down-Regulation of E-Cadherin Gene Expression by Collagen Type I and Type III in Pancreatic Cancer Cell Lines.* Cancer Research, 61(8):3508-3517.

Mayerle J, Schnekenburger J, Kruger B, Kellermann J, Ruthenburger M, Weiss FU, Nalli A, Domschke W, Lerch MM (2005) *Extracellular Cleavage of E-Cadherin by Leukocyte Elastase During Acute Experimental Pancreatitis in Rats.* Gastroenterology, 129(4):1251-1267.

Cha D, OB P, O'Toole EA, Woodley DT, Hudson LG (1996) *Enhanced modulation of keratinocyte motility by transforming growth factor-alpha (TGF-alpha) relative to epidermal growth factor (EGF).* Journal of Investigative Dermatology 106(4):590-597.

Sharpless NE, DePinho RA (2006)*The mighty mouse: genetically engineered mouse models in cancer drug development.* Nature Reviews: Drug Discovery, 5(9):741-754.

Frese KK, Tuveson DA (2008) *Maximizing mouse cancer models*. Nature Reviews Cancer, 7(9):654-658.

Hoffman R (2005) *Orthotopic metastatic (MetaMouse) models for discovery and development of novel chemotherapy.* Methods in Molecular Medicine, 111:297-322.

Johnson JI, S D, Zaharevitz D, Rubinstein LV, Venditti JM, Schepartz S, Kalyandrug S, Christian M, Arbuck S, Hollingshead M, Sausville EA (2001) *Relationships between drug activity in NCI preclinical in vitro and in vivo models and early clinical trials.* British Journal of Cancer, 84:1424-1431.

Lam SH, Chua HL, Gong Z, Lam TJ, Sin YM (2004) *Development and maturation of the immune system in zebrafish, Danio rerio: a gene expression profiling, in situ hybridization and immunological study.* Developmental & Comparative Immunology, 28(1):9-28.

Weiss L (1990) *Metastatic inefficiency.* Advances in Cancer Research, 54:159-211.

White RM, Sessa A, Burke C, Bowman T, LeBlanc J, Ceol C, Bourque C, Dovey M, Goessling W, Burns CE, Zon LI (2008) *Transparent Adult Zebrafish as a Tool for In Vivo Transplantation Analysis.* Cell Stem Cell, 2(2):183-189.